Vet Pathol **45**:140–153 (2008)

Detection of Antigenic Heterogeneity in Feline Coronavirus Nucleocapsid in Feline Pyogranulomatous Meningoencephalitis

L. Poncelet, A. Coppens, D. Peeters, E. Bianchi, C. K. Grant, and H. Kadhim

Anatomy/Embryology Department, Faculty of Medicine, Free University of Brussels, Bruxelles, Belgium (LP, AC); Clinical Sciences Department, Faculty of Veterinary Medicine, University of Liège, Liège, Belgium (DP); Animal Health Department, Faculty of Veterinary Medicine, University of Parma, Parma, Italy (EB); Custom Monoclonals International, Sacramento, CA (CG); and Anatomic Pathology Department; Neuropathology Unit, Brugmann University Hospital and Children Hospital, Free University of Brussels, Bruxelles, Belgium (HK)

Abstract. A new monoclonal antibody (mAb), CCV2-2, was compared with the widely used FIPV3-70 mAb, both directed against canine coronavirus (CCoV), as a diagnostic and research tool. Western blot showed that both anti-CCoV mAbs only reacted with a protein of 50 kD, a weight consistent with the feline coronavirus (FCoV) viral nucleocapsid. A competitive inhibition enzyme-linked immunosorbent assay showed that the 2 recognized epitopes are distinct. Preincubation of CCV2-2 mAb with FCoV antigen suppressed the immunostaining. Formalin-fixed, paraffin-embedded sections from brains of 15 cats with the dry form of feline infectious peritonitis (FIP) were examined by immunohistochemistry. Immunohistochemistry was performed with both anti-CCoV mAbs, either on consecutive or on the same sections. A myeloid-histiocytic marker, MAC 387, was also used to identify FIP virus–infected cells. In all regions where MAC 387–positive cells were present, positive staining with the CCV2-2 mAb was systematically detected, except at some levels in 1 cat. In contrast, none or only a few cells were positive for the FIPV3-70 mAb. Double immunostaining showed macrophages that were immunopositive for either CCV2-2 alone or alternatively for CCV2-2 and FIPV3-70 mAbs. This reveals the coexistence of 2 cohorts of phagocytes whose FIP viral contents differed by the presence or absence of the FIPV3-70–recognized epitope. These findings provide evidence for antigenic heterogeneity in coronavirus nucleocapsid protein in FIP lesions, a result that is in line with molecular observations. In addition, we provide for the first time morphologic depiction of viral variants distribution in these lesions.

Key words: Antigenic heterogeneity; cats; coronavirus; FIP; meningoencephalitis.

Introduction

Feline coronavirus (FCoV) is widely distributed in cats and other felids and causes endemic coronavirus infections that are mainly transmitted by the fecal-oral route. In the majority of infected cats, FCoV infection is mild or subclinical and limited to the gut. The infection is readily cleared in most cats, although shedding of infectious virus over protracted intervals may occur. In a minority of cats however, FCoV sometimes causes a severe, mostly fatal disseminated immune-mediated syndrome termed feline infectious peritonitis (FIP). Despite a generally high prevalence of FCoV infection in cats, particularly those in shelters and breeding colonies, FIP seemingly develops mostly in ''susceptible'' cats, particularly when the immune system is compromised, and/or when FCoV virulence is increased by mutational events.[12]

FCoV is an enveloped positive-stranded RNA virus of the family Coronaviridae. The 30-kb genome shares large homologies with other group I–related coronaviruses, including the canine coronavirus (CCoV) and the pig transmissible gastroenteritis virus.[6,26]

Coronaviruses generally have a strong potential for mutation. Point mutation, inversion, frame shift, and deletion have been demonstrated for FCoV,[15,37] and coronavirus RNA-RNA recombination has been reported in mice[18] and is suspected to occur in cats.[15]

Serologically, and by virus neutralization, FCoV has been subdivided into 2 serotypes (types I and II),[4,7] and type II FCoV seems to result from a recombination between FCoV type I and a CCoV.[15,25]

Two biotypes of FCoV are recognized: feline enteric coronavirus (FECV), which causes minimal disease, although some cats may shed the virus in feces over prolonged periods (possibly lifelong in some cases) and others clear the infection more readily.[1,2,8,10,14] The second biotype of FCoV is the feline infectious peritonitis virus (FIPV) that causes a severe systemic immune-inflammatory disorder characterized by typical pyogranulamatous lesions and vasculitis affecting many organs.[22] Such FIPV infections can present in 2 distinct clinical forms: the ''effusive'' (wet) form with intracavitary effusions and abdominal distension and the ''dry'' parenchymatous form with minimal effusion in serosal body cavities. In the latter case (dry form), neurologic involvement often occurs and is characterized by some as the ''neurologic'' or ''brain and eye'' form.[12,21,34]

Reverse transcriptase polymerase chain reaction (RT-PCR) amplification and product sequencing on RNA extracted from cat feces or rectal swabs have shown the emergence of genetic variants in the FCoV (FECV biotype) when sequential samples from the same cat are examined; similar results were obtained using samples from different cats within the same animal colony.[2,3,13,14] Such genetic drift seemingly takes place in the lower intestine, where FECV multiplies.[14] The DNA sequence variations between FECV and FIPV in samples obtained from a single cattery are less diverse than those found when the 2 viral biotypes are compared from different catteries.[2,14] FIPV biotype is thought to be derived from FECV biotype by mutation.[30,36] Serologic techniques, however, have so far failed to distinguish between cats harboring the FECV biotype and cats presenting with FIP.[28,29] In individual FIP symptomatic cats, molecular techniques (denaturating gel electrophoresis[11] or single-strand conformational polymorphism)[3] have revealed genomic differences in the FIPV, with different variants detected in different organs. These studies have provided evidence supporting the assumption that FIPV, like the FECV, may display genomic variations within the same individual animal.

In the present study, tissues were removed from cats presenting with the typical clinical and histopathologic dry form of FIP. Two anti-CCoV mAb were compared as immunohistochemical (IHC) diagnostic tools; 1 (designated FIPV3-70) has been demonstrated as a valuable diagnostic agent for FIP diagnosis,[21] and the other (designated CCV2-2) is a new anti-CCoV clone. Reducing Western blot showed that both mAbs targeted the same protein with a molecular weight consistent with the FIPV nucleocapsid (N) protein. Consequently, our methods facilitated studies of the presence of antigenic N protein heterogeneity even within single lesions, and such investigations complement previous reported occurrences of genomic variations in FIPV occurring within tissues from the same infected animal.

Materials and Methods

Animals

Fifteen cats with progressive neurologic disorders compatible with diffuse or multifocal central nervous system involvement were included in this study (Table 1); they were eventually euthanized, and tissues were examined histologically. Inclusion criteria were based on the histopathologic findings, including the FIP-typical phlebitis and periphlebitis of the leptomeninges.[22,33] Elevated serum total protein level and low albumin/globulin ratio, intracavitary effusion, and granulomatous lesions in other organs were noted as additional diagnostic evidence. Eight of the subjects were purebred cats and 7 mixed breeds; 10 were males and 5 females; 9 were less than 1 year of age at presentation, and all but 1 (No. 14) were less than 4 years of age. All cats had ataxia of all 4 limbs that worsened over a period of 3 to 4 weeks and was later compounded by altered consciousness, compulsive walking, epileptic fits, or decerebrate rigidity in some cases (Table 1). Three cats (Nos. 2, 10, and 15), in addition, displayed unilateral iridocyclitis. Serum protein level and serum albumin/globulin ratio were evaluated in most cases, and results are reported in Table 1. Two kittens (Nos. 5 and 7) were siblings from a same litter and had not been in contact with other cats aside from their parents and littermates. The brains of all the cats were removed and immersed in 10% formalin within 60 minutes of euthanasia. The affected eye from 2 cats (Nos. 2 and 10) with ocular inflammatory changes was processed under the same conditions, as were samples of kidneys with granulomatous lesions from 2 cats (Nos. 2 and 12). Two additional cats were included as controls; 1 presented the typical exudative abdominal form of FIP and was used as a positive control. The second cat was healthy and had neither neurologic signs nor FIP-related lesions. Parts of these control serosal lining samples were either formalin-fixed (for IHC staining) or snap frozen in liquid nitrogen and then stored at −80°C (for Western blot).

Histopathology

After 5 days in the fixative, samples were immersed in 0.1 M phosphate-buffered saline (PBS) for 2 to 5 days. Brains were divided along the sagittal plane; the right half was stored in 0.1 M PBS, at 4°C and the left half divided into 10 blocks along transverse planes at fixed landmarks. The blocks (including serosal lining controls) were routinely processed for paraffin embedding and cut at 6 μm. Brain sections were stained with luxol fast blue/cresyl violet and with hematoxylin/eosin (HE); sections from other tissues were stained with HE.

Table 1. Characteristics of the 15 cats enrolled in this study. Normal range for serum protein (Prot.) is from 5.7 to 7.3 g%. Albumin to globulin ratio (Alb./Glob.) at or below 0.7 is viewed as suggesting feline infectious peritonitis diagnosis.

Cat No.	Breed	Age (months or years)	Sex	Main Clinical Findings on Presentation	Prot. (g %)	Alb./Glob.	Main Pathologic Findings
1	Birman	8 m	F	Ataxia, paresis	9.4	0.61	Meningitis
2	Mongrel	4 m	M	Fever, obtunation, iritis, ataxia, paresis	ND*	ND	Meningitis, lateral ventricules enlargement, granulomatous peritonitis, granulomatous nephritis
3	Mongrel	7 m	M	Obtunation, spastic tetraplegia	ND	ND	Meningitis, lateral ventricules enlargement
4	Mongrel	3 y	M	Obtunation, head bobbing, no occulocepahlic reflex, spastic tetraparesis	7.1	ND	Meningitis
5	Birman	3 m	M	Ataxia, paresis	ND	ND	Meningitis
6	Maine Coon	7 m	M	Obtunation, head bobbing, no occulocepahalic reflex, hypermetria, delayed placing reflexes	ND	ND	Meningitis, exudative pleurisy
7	Birman	4 m	M	Ataxia, paresis	8.6	0.45	Meningitis
8	British Short Hair	18 m	F	Obtunation, compulsive walking, poor equilibrium, 1 epileptiform fit	9.3	0.45	Meningitis, granulomatous hepatitis
9	Mongrel	15 m	M	Comatous, spastic tetraplegia, emphrostotonos, no placement reflexes	7.9	1.22	Meningitis, severe hydrocephalus
10	Birman	18 m	M	Ataxia, paresis, iritis	12	0.23	Meningitis
11	Birman	9 m	F	Obtunation, head bobbing, ataxia, paresis, epileptiform fits	8	0.6	Meningitis
12	Mongrel	4 m	M	Fever, ataxia, paresis	10	0.4	Meningitis, granulomatous nephritis
13	Persian	4 m	F	Obtunation, ataxia, paresis, poor menace response	7.3	0.69	Meningitis
14	Mongrel	13 y	F	Obtunation, ataxia, paresis, poor menace response	ND	ND	Meningitis
15	Maine Coon	12 m	M	Fever, obtunation, iritis, poor placing reactions	8.1	0.9	Meningitis

* ND = not determined.

Immunohistochemical techniques

FIPV3-70 and CCV2-2 mAbs were obtained from Custom Monoclonals International (West Sacramento, CA). Both mAbs were made by immunizing Balb/c mice with canine coronavirus (CCoV, strain CCV51). The epitopes recognized by these antibodies are unknown. The original concentration of these mAbs was 4.5 mg/ml and 4.1 mg/ml, respectively. At least 2 tissue blocks exhibiting typical histopathologic changes were selected for IHC investigations from each cat. Adjacent sections were treated with either FIPV3-70 or CCV2-2 mAbs; in addition, sections from both positive and negative (FIPV3-70 or CCV2-2 mAbs treated) cases were also tested with MAC 387 antihuman myeloid/histiocyte antigen mAb (Serotec, Oxford, UK).

For optimal FIPV3-70 mAb staining, we found it best to preheat sections (close to boiling point) in 0.01 M citrate buffer for 20 minutes in a microwave before the primary antibody. CCV2-2 mAb did not require any pretreatment for epitope retrieval (pretreatment as

described for FIPV3-70 did not modify CCV2-2 reactivity, however).

MAC 387 antibody reaction required 15 minutes of preincubation at 37°C with 0.1% trypsine and 0.1% $CaCl_2$ solution (as suggested by the supplier).

Dewaxed sections were rinsed; nonspecific binding was blocked by incubating the slides with 1/20 normal sheep serum (NSS) for 15 minutes. Incubation with the primary mAb (FIPV3-70 diluted to 1/400, CCV2-2 at 1/600, and MAC 387 at 1/1000 all in 1/100 NSS) occurred for 12 to 36 hours at 4°C. Sections were rinsed, incubated with 1/20 NSS, and then with goat antimouse immunoglobulin serum at 1/80 in 1/100 NSS as secondary antibody for 15 minutes. Slides were rinsed then incubated for 15 minutes with peroxidase-antiperoxidase complex 1/300 in 0.01 M PBS for 15 minutes. After rinsing, the presence of antigen was revealed with DAB-H_2O_2 solution (liquid DAB substrate pack from Biogenex, San Ramon, CA), which resulted in a brown deposit. The sections were lightly counterstained with hematoxylin, dehydrated, and mounted.

Sections from up to 10 blocks, negative for FIPV3-70 mAb, were further processed. Thus, sections were first screened immunohistochemically using FIPV3-70 as the primary antibody (as described above). Then, CCV2-2 mAb was applied (as the other primary antibody) on the same section. This second reaction was revealed using DAB in Tris/Nickel buffer with 0.1% H_2O_2 as chromogen, which resulted in blue staining. These successive immunostainings were also conducted with the same mAbs used in reverse order, that is, CCV2-2 first followed by FIPV3-70.

Double immunofluorescent staining was also carried out on tissue blocks positive for both mAbs on adjacent sections, using biotinylated horse antimouse secondary antibody (1/100 in 1/100 NSS), after blocking the endogenous biotin (Avidin/biotin blocking kit, Vector, Burlingame, CA). Color development was conducted with Alexa 594–coupled streptavidine after incubation with FIPV3-70 mAb (red fluorescence) and with Alexa 488 coupled–streptavidine after incubation with CCV2-2 mAb (green fluorescence). Both fluorochromes were obtained from Molecular Probe (Carlsbad, CA) and diluted at 1/100 in 0.01 M PBS. Slides were mounted with an aqueous medium (Vectashield, Vector) and analyzed with a fluorescent microscope.

In all immunostaining runs, slides in which the primary antibody step was skipped or replaced by an irrelevant mAb served as negative controls. Positive controls were also systematically included: sections from the serosal lining of the control cat with the abdominal exudative FIP (this tissue stained positive for both FIPV3-70 and CCV2-2 mAbs) for FCoVstaining and sections from a feline mesenteric lymph node for MAC 387 staining.

Reducing Western blots

The Western blot technique was used to evaluate the specificity of the 2 mAbs on 2 sources of viral antigens: 1 from a laboratory strain of the CCoV (isolate CCV51 adapted to grow in Crandell feline kidney [CrFK] cells, a gift from L. E. Carmichael at the Barker institute for Animal Health, Cornell University, to C. K. G.) and the other from a field virus from a diseased cat.

The CCV51 coronavirus isolate was grown in confluent monolayers of CrFK cells, and the virus plus cell debris was harvested at the stage of syncytial cell formation. The culture mixture was snap frozen and thawed and then spun at 1,500 × *g* to remove cellular debris; clarified supernatant was then ultracentrifuge pelleted (110,000 × *g* for 90 minutes using a swinging bucket rotor). The virus pellets so obtained were pooled, washed once using PBS pH 7.4, and then resuspended in PBS (positive control). For noninfected CrFK membranes, uninfected cell cultures were treated identically (negative control).

For the feline virus, frozen granulomatous serosal lining from the control cat with the typical form of abdominal exudative FIP was processed. This same tissue tested positive (FIP+) with both mAbs, namely FIPV3-70 and CCV2-2, in IHC preparations.

Serosal lining from a healthy control cat was also collected, which tested negative (FIP-) for the same mAbs.

The frozen samples from the healthy and diseased control cats were mechanically homogenized in 5 volumes of a Tris-HCL buffer (10 mM, ph 7.4) containing 5 µl/ml aprotinin 10% (Sigma, Providence, RI) and 5 µl/ml phenylmethylsulfonyl fluoride (1.74 mg/ml isopropanol). Total protein was measured using a colorimetric procedure (BCA Protein Assay Kit, Pierce, Rockford, IL) and was found to be 2.65 mg/ml and 13.7 mg/ml for the positive and negative control preparations, respectively, and 101 mg/ml and 97 mg/ml for FIP+ and FIP- samples, respectively.

Virus and negative control preparations were diluted in 4 volumes of Tris-HCL buffer (0.5 M, pH 6.8) containing 0.1 g/ml sodium dodecyl sulfate (SDS; Sigma), 0.1 mg/ml beta mercaptoethanol 20%, 0.5 g sucrose, and 0.1 ml bromophenol blue and were boiled for 5 minutes. The total amount of proteins loaded on a gel-loading surface was 150 µg for FIP+, 162 µg for FIP-, 40 µg for negative control, and 5.76 µg for positive control.

The nonspecific lane was loaded with FIP+ (150 µg). Samples were subjected to electrophoresis (75 minutes, 150 V) in a Tris-glycine discontinuous SDS-polyacrylamide gel (4 % stacking gel, 10% separating gel). After semidry protein transfer (60 minutes, 100 mA), the nitrocellulose membranes were saturated for 2 hours in Tris-HCl buffer (10 mM, pH 7.4) containing 10% powdered fat-free milk and 0.2% Tween 20 (Sigma). The blots were incubated (in 15 ml/blot) overnight with either FIPV3-70 or CCV2-2 mAb diluted (15 µg/ml) in 2% bovine serum albumin buffer (BSA; Sigma). The nonspecific control blot lane was incubated in the 2% BSA buffer. The blots were washed 4 times, 15 minutes each, with 0.2% Tween 20 buffer and incubated for 2 hours (15 ml/blot) with 1/2000 antimouse IgG alkaline phosphatase conjugate (Sigma) in 2% BSA buffer. Staining was performed in 100 mM Tris (pH 9.5)

containing 100 mM NaCl, 5 mM $MgCl_2$, bromochloroindolyl phosphate (3.5 µl/ml), and nitro blue tetrazolium substrates (4.5 µl/ml) (Sigma).

Molecular weights of proteins recognized by the mAbs were determined by comparison with either prestained low- and high-range molecular weights standards (Amersham, Life Sciences, UK) or the SDS-6B molecular weight range (Sigma).

Antigen-antibody preincubation

A concentrate source of FCoV was prepared by diluting 57 doses of Primucel (Pfizer, Brussels, Belgium) vaccine; they were first centrifuged at 4,000 rpm to remove cellular debris; the supernatants was then centrifuged at 100,000 × *g* for 2 hours; the pellets were resuspended in 400 µl PBS 0.01 M and sonicated for 30 seconds. The antigen suspension was used as such or diluted at 1/10, 1/100, and 1/1,000 in PBS 0.01 M. These 4 antigen suspensions were mixed overnight at 4°C with CCV2-2 and NSS; the final mAb and NSS concentrations in the mixtures were the same as that of the CCV2-2 mAb solution used in the histopathologic study. On serial sections from a CCV2-2–positive block, the mixtures replaced the primary antibody in the immunostaining process.

Competitive inhibition enzyme-linked immunosorbent assay

CCoV and FCoV (serotype II) were produced in cell culture using CrFK cells. All enzyme-linked immunosorbent assay (ELISA) operations were carried out at room temperature. Immulon II HB (Thermo, Milford, MA) were coated overnight with 250 ng ultracentrifuge-sedimented whole coronavirus protein in PBS, pH 7.2; plates were then washed twice with saline and tap dried. ELISA buffer (0.15 M NaCl; 0.05 M Tris-HCl; 1 mM EDTA; 3% BSA fraction V, 3.5% fetal calf serum, and 0.05% Tween 20, pH 7.4) was added to all wells (80 µl in wells in which nonbiotin conjugated mAb was to be added or 100 µl for other wells). Nonconjugated mAb (SpA purified) was added at 5.0 µg/well in 20 µl where required, then biotin conjugated mAb was added at 2.0 µg/well to the first well of each row, and the volume in the first well was brought to a total of 200 µl total volume. The biotinylated mAb was then double diluted over 8 wells, resulting in a dilution series from 1,000 ng/100 µl in the first well to 8 ng/100 µl in the last (eighth) well. Simultaneously, the ratio of biotin-conjugated mAb to competitor, unconjugated mAB in the first well was 1 : 5, and this effectively decreased to 1 : 640 in the last well. Plates were incubated for 45 minutes, washed 3 times, and tap dried. Avidin-peroxidase (ExtrAvidin, Sigma E-2886) was diluted 1:1,000 in ELISA buffer and 100 µl/well added; plates were incubated 45 minutes and then washed 3 times and tap dried. Substrate (15 ml/plate for 150 µl per well) was o-Phenylenediamine (Sigma, P-1526): 20 mg dissolved in 15 ml of 50 mM citric acid and 100 mM dibasic sodium phosphate pH 5.0, activated with 80 µl per plate hydrogen peroxide (30% solution, Fisher Scientific, Waltham, MA). The reaction proceeded for 8 minutes and was then stopped by addition of 50 µl/well 2.0 M sulphuric acid. The reaction color was read at 493 nm.

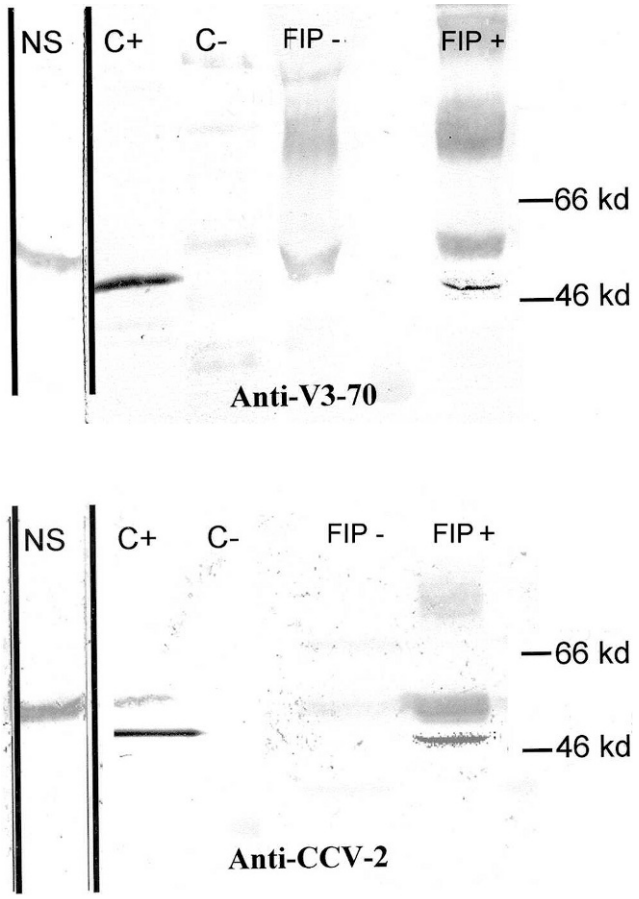

Fig. 1. Western blots for the 2 mAbs (FIPV3-70 and CCV2-2) used in our study: C+: supernatant from CCoV-infected Crandell feline kidney (CrFK) cell culture; C- supernatant from uninfected CrFK cell culture; FIP+: whole extract from the granulomatous intestinal serosal lining from a cat with typical abdominal exudative FIP form; FIP-: whole extract from serosal lining from a control cat; NS: nonspecific lane loaded with FIP+ extract and incubated in 2% BSA buffer without first antibody.

Results

Reducing Western blots revealed that both anti-CCoV mAbs (FIPV3-70 and CCV2-2) reacted with a protein of approximately 50 kD, when the virus was ultracentrifuge sedimented from CCoV-infected cell culture supernatant, and also with a similar sized band when the virus was derived from infected cat serosal tissues (Fig. 1). This molecular

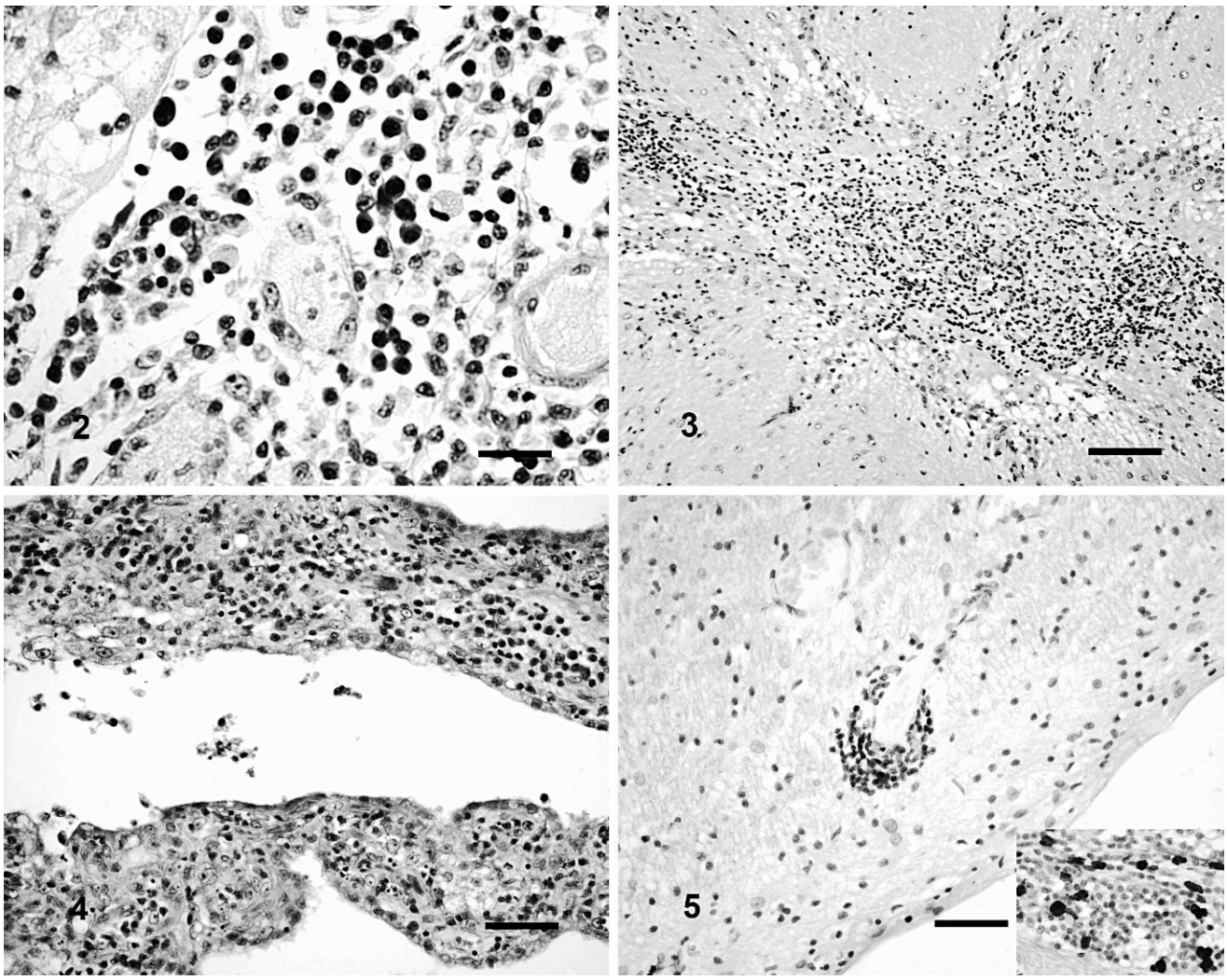

Fig. 2. Main FIPV cerebral lesions. Ventral aspect of the medulla leptomeninges, cat No. 5: pleiomorphic infiltrate including lymphocytes, plasma cells, macrophages, and polymorphonuclear cells; hematoxylin and eosin. Bar: 25 μm.

Fig. 3. Main FIPV cerebral lesions. Hypothalamus, cat No. 9: parenchymatous inflammatory cell invasion; hematoxylin and eosin. Bar: 100 μm.

Fig. 4. Main FIPV cerebral lesions. Fourth ventricle choroid plexus, cat No. 9: inflammatory cell infiltration; hematoxylin and eosin. Bar: 50 μm.

Fig. 5. Main FIPV cerebral lesions. Vicinity of the lateral ventricle, cat No. 3: perivascular lymphocytes; no positivity with the CCV2-2 antibody. Inset: leptomeninges of the fourth ventricule of the same cat, including macrophages darkly stained with the MCA 387 antibody. PAP method, diaminobenzidine visualization, lightly countercolored with hematoxylin. Bar: 50 μm.

weight is compatible with the FCoV nucleocapsid protein (N).[27]

Examination of the brain in the 15 cats showed the typical histopathologic changes required for inclusion in this study. The leptomeninges were infiltrated by pleiomorphic inflammatory cells consisting of lymphocytes, plasma cells, macrophages, and polymorphonuclear neutrophils (Fig. 2). The vascular changes recently detailed were recognized, including monocyte adherence to small vein walls, intravascular monocyte accumulation, local vein wall disruption, and local or privascular granulomatous formation (Fig. 3).[22]

Pyogranulomatous lesions occasionally exhibited necrotic centers. The infiltrate was most prominent on the ventral aspect of the caudal brainstem. However, discrete foci of periphlebitis were occasionally seen in the regions of the optic chiasma and the telencephalic leptomeninges. Infiltrates often invaded the subjacent neural parenchyma, particularly along the perivascular spaces, resulting in the formation of ''perivascular cuffs'' at several

sites. In 1 cat an extensive parenchymal infiltrate was seen at the level of the hypothalamus (Fig. 3). Choroid plexi were also involved (Fig. 4), particularly in the fourth ventricle, which was the most affected. Some degree of lateral ventricular enlargement was observed in 2 cats, while 1 cat had severe hydrocephalus (Table 1). Perivascular lymphocytic infiltrates were also found in structures bordering the lateral ventricles, mostly in the caudate nucleus (Fig. 5). In the 2 cases in which the eyes were studied, isolated inflammatory lesions could be found in the vascular layer. Tissue blocks with severe inflammatory lesions were used for IHC.

IHC staining using MAC 387 antibody showed numerous positive cells with typical morphology of macrophages in all cats. These cells were particularly abundant in the leptomeninges, choroid plexi, and perivascular spaces. In these lesions, analysis of adjacent sections revealed that cells with these morphologic characteristics were systematically stained positive by the CCV2-2 mAb in all cat tissues, including cells in all cerebral structures examined, in the 2 eyes, and in the 2 kidneys studied. The only exception was cat No. 13, in which few positive cells were retrieved.

On the contrary, FIPV3-70–positive cells (also with monocyte/macrophage morphology) were observed in only 7 of the 15 cats (Fig. 6, Table 2). In addition, in 5 of the 7 FIPV3-70–positive cats, not all cerebral structures were positive for FIPV3-70. Generally, analysis of adjacent sections showed that FIPV3-70 immune-positive cells (in the 7 positive cats) were less abundant than CCV2-2–positive cells (Fig. 6c, d). In addition, lesions in different cerebral structures were FIPV3-70 positive in 1 male sibling (cat No. 7), whereas for the other male littermate (cat #5), the cerebral lesions were negative. Staining with CCV2-2 and FIPV3-70 mAbs was restricted to the cytoplasm of the positive cells.

Data in Table 2 show that the pattern of immune detection or lack thereof for the 2 coronavirus epitopes (as comparatively stained by either CCV2-2 or FIPV3-70) in various lesions was the same in some animals (Nos. 1, 4, 5, 7, 9, 11, 12, and 14), whereas it was different in others (Nos. 2, 3, 6, 8, 10, 13, and 15). In 2 of the cats this dissimilarity was found to be tissue specific: between the eye and the brain (Nos. 2 and 10) and between the kidney and the brain (No. 2).

Examination of 3 telencephalic paraventricular regions in which lymphocytic infiltration was noted (particularly in the caudate nucleus) showed absence of staining with either of the anticoronavirus antibodies. MAC 387–positive cells were also absent in these regions (Fig. 5). Besides IHC on serial sections, we did double IHC staining. On sections negative with FIPV3-70 mAb, FIPV antigen was subsequently revealed incubating with CCV2-2 mAb. Sections containing FIPV3-70–positive cells showed, besides, the presence of CCV2-2–positive cells (Fig. 7). In instances in which a section was positive with FIPV3-70 mAb on single IHC, when doing double IHC and applying CCV2-2 mAb first, no additional FIPV3-70–positive cells could be detected. Cells including the FIPV3-70–recognized epitope alone were not observed.

In summary, these results indicate that coronavirus antigens stained by FIPV3-70 and/or CCV2-2 assort in 2 distinct patterns in macrophages/monocytes: viral particles that are stained exclusively by CCV2-2 and viral particles that are stained by both anticoronavirus mAbs. Usually, the 2 immunologically distinct cell cohorts detected in our double immune-staining technique were segregated, although occasionally the 2 cellular cohorts were found intermingled (Fig. 6).

Preincubation of the CCV2-2 mAb with the FCoV antigen induced a dose-dependent reduction of the immunostaining on serial sections from a positive block (Fig. 8). The results of the ELISA tests run to detect inhibition of binding of FIPV3-70 by CCV2-2 (or vice versa) on either FCoV serotype II or CCoV are shown in Fig. 9; SD on 3 repeats of each point (mean) ranged from 6 to 234 optical units. The figure demonstrates that purified (but nonconjugated) FIPV3-70 mAb significantly inhibited the binding of biotin-conjugated FIPV3-70 mAb on CCoV or FCoV even at a ratio of 5 : 1; the inhibition of mAb binding became more marked as the native to conjugated mAb ratio increased. Nonconjugated CCV2-2 mAb, however, had no effect on the binding of FIPV3-70-biotin, even at the highest ratio used of 640 : 1. Similarly, native CCV2-2 mAb significantly inhibited binding of biotin-conjugated CCV2-2 mAb but had no effect on the binding of biotinylated FIPV3-70 mAb on either the cat- or the dog-purified coronavirus isolates.

Discussion

This study shows the coexistence of 2 cohorts of phagocytes whose FIP viral contents differ by the presence or absence of the FIPV3-70 epitope. This was inferred by the detection of macrophages that were labeled either by CCV2-2 mAb alone or by both CCV2-2 and FIPV3-70 mAbs. It shows the presence of at least 2 FIPV populations differing by 1 epitope of the viral nucleocapsid (N) protein in FIPV-infected felines.

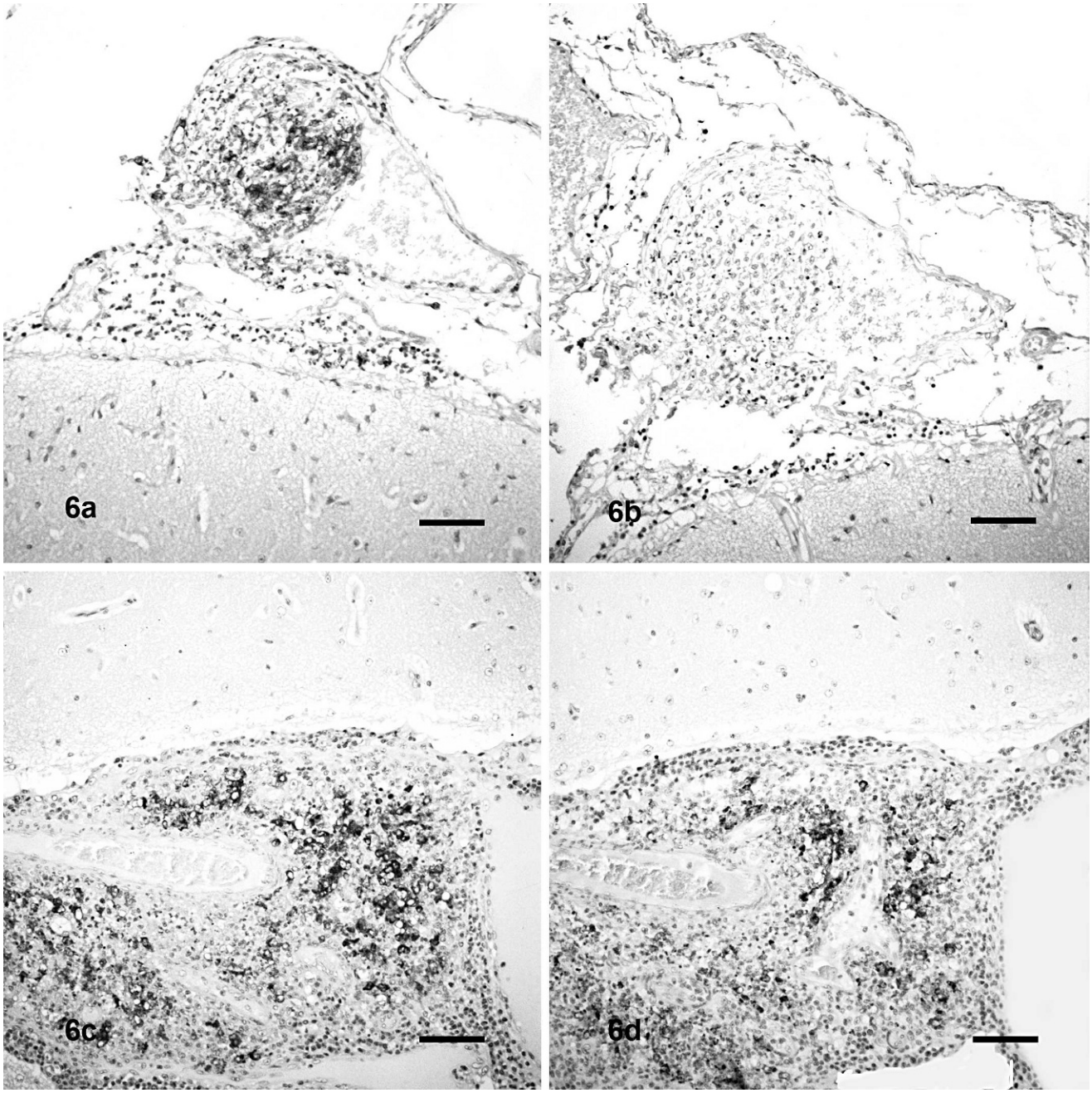

Fig. 6. Comparative study of anti-CCoV mAbs immunoreactivity in the brain: Adjacent sections showing inflamed medulla leptomeninges (upper row) and perivascular inflammation (lower row). a, b from cat No. 3 and c, d from cat No. 7. a, c reacted with the CCV2-2 monoclonal antibody; b, d reacted with the FIPV3-70 monoclonal antibody: cat No. 3 is FIPV3-70 negative and CCV2-2 positive, whereas cat No. 7 is positive with both antibodies. PAP method, diaminobenzidine visualization, light hematoxylin counterstaining. Bar: 100 μm.

Findings thus provide a morphologic documentation for this viral diversity in FIPV lesions/pathology. Our results also showed the presence of different viral variants among kittens from the same litter, among organs (eyes, kidney, and brain) in the same animal, among different affected structures and levels of the brain, and among macrophages from the same lesion. The coexistence of different variants of FIPV in diseased cat tissues has been reported by others using genomic techniques, including denaturating gel electrophoresis on amplicons from spike (S) and N genes,[11] and single-strand conformational polymorphism on N gene and open reading frame 7b amplicons.[3,23] It is worth noting that coronavirus N protein conservation is known to be low.[24]

Table 2. Immunoreactivity with feline infectious peritonitis V3-70 and CCV2-2 monoclonal antibodies at different levels of the central nervous system, eye balls, or kidney of the 15 diseased cats enrolled in this study. Caudal, middle, and rostral medulla levels correspond to the spinal cord–medulla junction, inferior olive, and superior olive levels, respectively.

Cat No.	Level	FIPV3-70	CCV2-2
1	Caudal medulla	-	+
	Middle medulla	-	+
	Thalamus	-	+
2	Eye	-	+
	Middle medulla	+	+
	Thalamus	+	+
	Kidney	-	+
3	Middle medulla	-	+
	Thalamus	-	+
	Basal nuclei	+	+
4	Cervical Spinal Cord	-	+
	Caudal medulla	-	+
	Middle medulla	-	+
5	Caudal medulla	-	+
	Middle medulla	-	+
	Pons	-	+
6	Caudal medulla	+	+
	Rostral medulla	-	+
	Mesencephalon	-	+
7	Caudal medulla	+	+
	Middle medulla	+	+
	Frontal lobe	+	+
8	Mesencephalon	-	+
	Basal nuclei	+	+
9	Rostral medulla	-	+
	Basal nuclei	-	+
10	Eye	-	+
	Rostral medulla	+	+
	Mesencephalon	-	+
11	Caudal medulla	-	+
	Middle medulla	-	+
	Rostral medulla	-	+
12	Caudal medulla	+	+
	Rostral medulla	+	+
	Mesencephalon	+	+
	Kidney	+	+
13	Caudal medulla	-	+
	Middle medulla	-	-
	Rostral medulla	-	+
	Pons	-	-
	Mesencephalon	-	-
14	Cervical spinal cord	-	+
	Caudal medulla	-	+
	Rostral medulla	-	+
	Mesencephalon	-	+
15	Caudal medulla	-	+
	Rostral medulla	+	+
	Caudal colliculus	+	+
	Rostral colliculus	+	+
	Thalamus	+	+
	Caudate	+	+

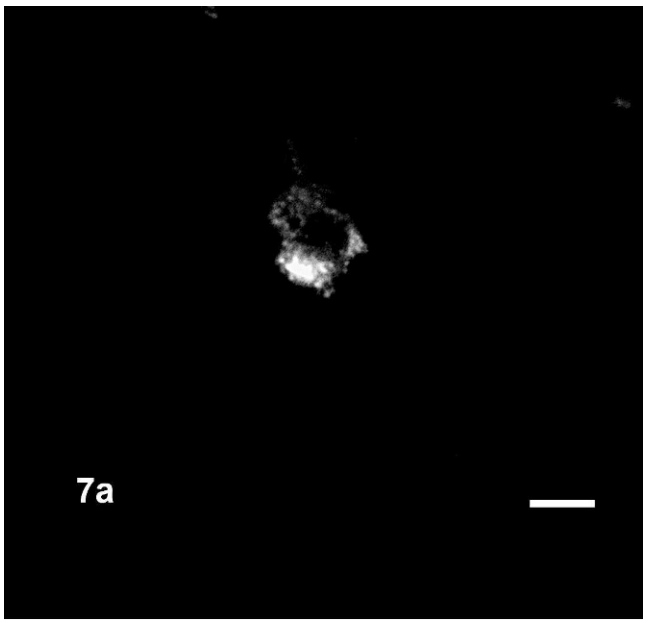

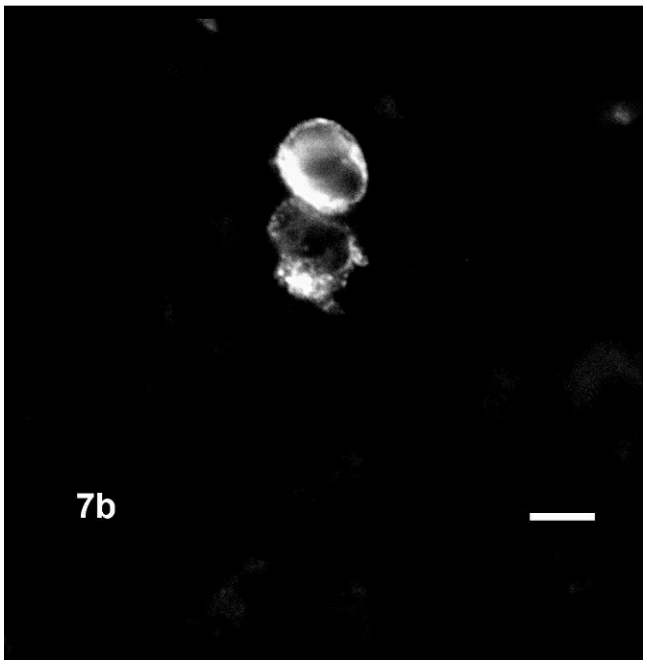

Fig. 7. Medulla leptomeninges, cat No. 10: reaction with FIPV3-70 antibody reveals a positive macrophage; subsequent reaction with CCV2-2 antibody reveals a second macrophage in close contact with the first one. Double immunofluorescent staining, streptavidine-biotine method. Bar: 5 μm.

The present study took a different approach, demonstrating heterogeneity at a viral protein level, namely the N protein, with IHC. These results complement those obtained using molecular techniques. In addition, our methods make it possible to obtain new information about the topographic distribution of these viral variants in affected animals, whereas molecular techniques cannot

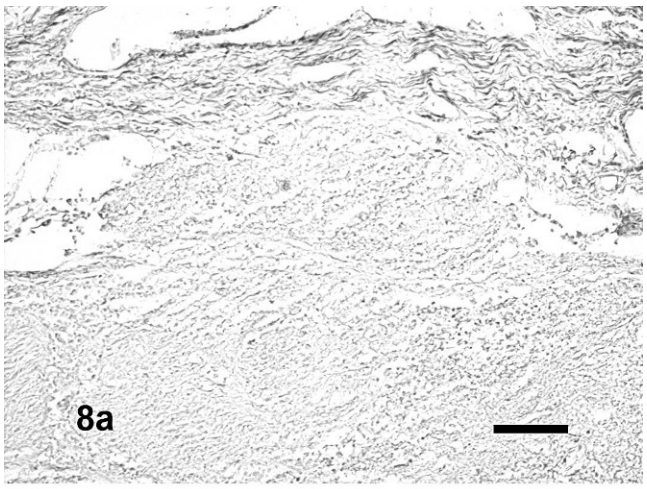

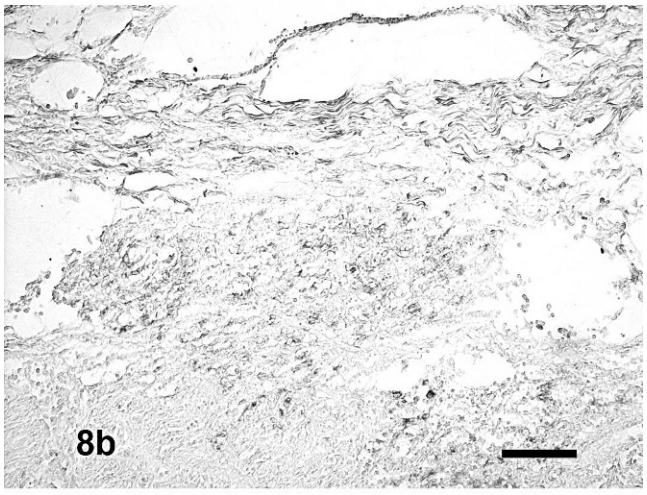

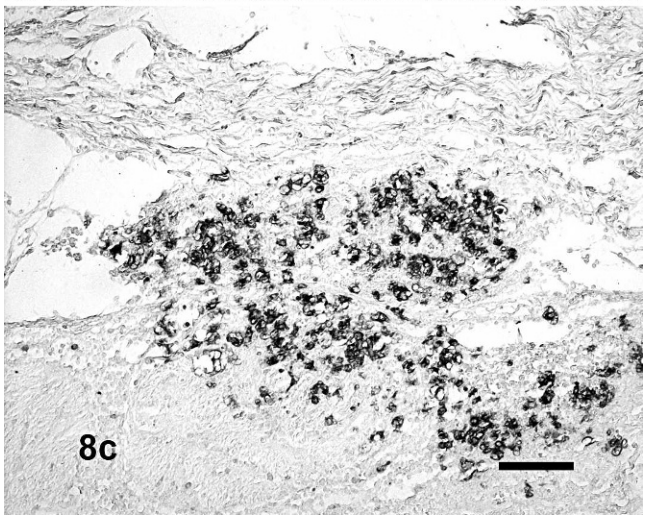

Fig. 8. Medulla leptomeninges, cat No. 12, serial sections from a CCV2-2–positive block; a, b, c, primary antibody incubated with FCoV particle suspensions diluted at 1/10, 1/100 and 1/1,000, respectively. Macrophage immunostaining is suppressed in a dose-dependent manner by preincubation of the antibody with the antigen. PAP method, diaminobenzidine visualization, no counterstaining. Bar: 50 μm.

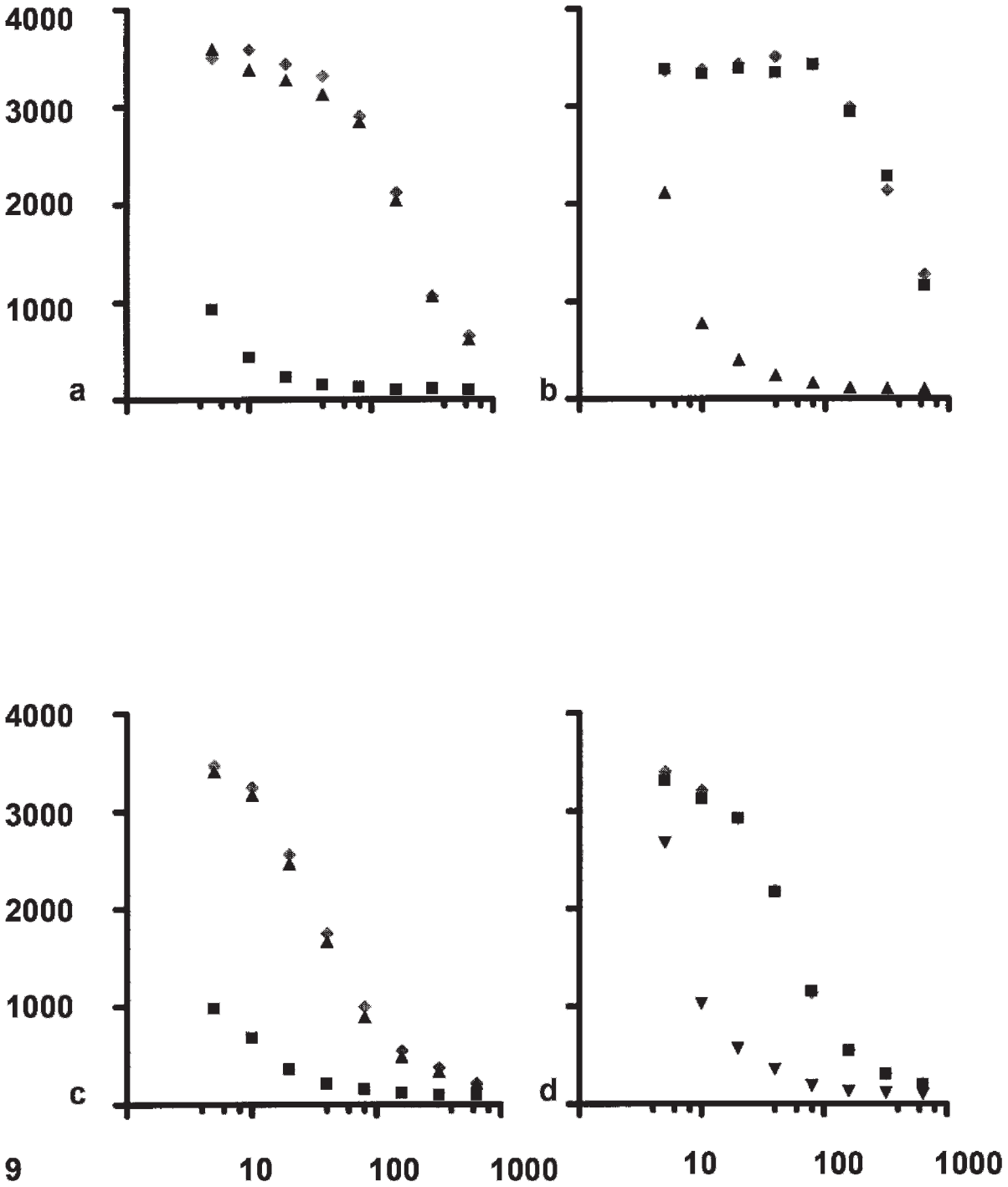

Fig. 9. ELISA competition assays conducted on CCoV-coated wells (6a, b) or FCoV (serotype II)-coated wells (6c, d); either virus reacted with biotinylated FIPV3-70 mAb (6a, c) or biotinylated CCV2-2 mAb (6b, d). Ordinate: optical density at 493 nm of the biotinylated mAb-antigen complexes (phenylenediamine, H_2O_2 revelation). Abcissa: successive ratio of biotinylated mAb to competitor mAb from 1/5 to 1/640, also the successive double dilutions of the biotin-conjugated mAb from 1 µg/100 µl to 8 ng/100 µl. Biotinylated mAb reacted in the absence (diamonds) or in the presence of a 5-µg/200-µl well of competitor unconjugated mAb (squares: FIPV3-70, triangles: CCV2-2).

detect detail distribution of viral genome because they rely on homogenates.[3,11,23]

It should be kept in mind that other processes, different from genomic changes, may be involved in N protein epitope alteration, namely alternative splicing and post-translational protein modifications. Alternative splicing as a cause of epitope change in FCoV could be excluded because plus-strand RNA synthesis sensitivity to ultraviolet light was found to be proportional to RNA length, ruling out splicing in subgenomic RNA formation in coronavirus species, namely, mouse hepatitis and infectious bronchitis coronaviruses.[16,33] Post-translational coronavirus N protein modification could, however, not be completely excluded as a cause of epitope change. The coronavirus N protein has high serine content and is extensively phosphorylated.[24] In one study, the N protein of the infectious bronchitis virus showed different degrees of phosphorylation in cell lysates from different cultured cell lines.[17] Surprisingly, virions in the cell culture supernatants contained the same hyperphosphorylated N protein regardless of the cell line used.[17] In such experimental conditions, a change in the cytoplasmic N protein epitope resulting from the varying degrees of phosphorylation remains a possibility. However, N protein phosphorylation occurs in both the cytoplasm and the nucleus, as was detected notably in severe acute respiratory syndrome (SARS) coronavirus; successful translocation of the N protein from infected cells nuclei towards their cytoplasm relies on N protein phosphorylation.[35] Our finding of N protein IHC strict localization to the cytoplasm of infected macrophages reflects successful nuclear-to-cytoplasmic translocation and suggests adequate phosphorilation.[35]

It is generally believed that macrophage invasion is the key factor by which the FIPV escapes immune defence mechanisms. These virus-laden phagocytes provide a vehicle for virus dissemination and replication.[5,33,38] Macrophages also trigger the FIP-specific granulomatous vasculitis.[22]

Thus, the virus seems to resist digestion by macrophages, and its replication would induce an endless immune inflammatory reaction. Our finding of viral antigenic heterogeneity within such lesions suggests, however, that additional mechanisms by which FIPV can escape host defences and deregulate inflammatory reaction, like antigenic drift, may also play a role in this entity. Viral antigenic drift is indeed known to be implicated in some severe inflammatory diseases, such as viral hepatitis C in humans.[9,31]

The coronavirus N protein (despite not being a surface protein) still remains a relevant factor in the immunopathogenicity of FIP. It is indeed one of the most abundant structural proteins of coronaviruses and can trigger vigorous humoral and cellular immune responses to the point that it has been considered for production of a SARS vaccine.[20] It is worth noting that the amino acid sequence and localization within the FCoV N protein of both epitopes targeted by the 2 mAbs used in this study remain unknown. Nevertheless, the CCV2-2–recognized epitope seems more frequent than the FIPV3-70–recognized epitope in FIPV. Further molecular studies are thus worth undertaking to disclose these molecular characteristics because viral molecular changes associated with FIP disease remains a very challenging question.[19,32]

Our results showed that in the 15 cats presenting the typical clinical and pathologic picture of the dry form of FIP, CCV2-2 positivity in macrophages was always detected in lesions with MAC 387–positive cells. Thus, 46 of 49 samples stained positive with the CCV2-2 mAb, yielding a sensitivity of 94% for this mAb. On the contrary, only 18 of the 49 samples showed FIPV3-70 positivity in macrophages, implying 37% sensitivity.

It is noteworthy that the Western blot specificity of both mAbs was excellent, as evidenced by the observation of a single band in the positive lanes of the Western blots. In the formalin-fixed/paraffin-embedded sample, specificity was further evidenced by the strict restriction of the positive reaction to the cytoplasm of some macrophages of diseased cats and by the extinction of the immunostaining by preincubation of the CCV2-2 mAb with the FCoV antigen. The high sensitivity of CCV2-2 mAb highlights its potential usefulness in confirming FIPV diagnosis and in research. The fact that antigen retrieval treatment is not required for IHC is also an advantage for CCV2-2 mAb.

The ELISA to demonstrate competitive inhibition of binding showed that the nucleocapsid epitopes bound by FIPV3-70 and by CCV2-2 (on either canine or feline coronaviruses) are totally distinct and nonoverlapping. The disparate epitopes appear to be sufficiently separated that no spatial inhibition of binding was detected, even when the available binding sites were saturated by 1 or the other mAb.

Acknowledgements

This study was supported by a grant from the Fonds National de la Recherche Scientifique (# 1.5025.02) to L. P. We thank Pfizer Belgium for providing the Primucell vaccine.

References

1 Addie DD, Jarret O: Use of a reverse transcriptase polymerase chain reaction for monitoring the shedding of feline coronavirus by healthy cats. Vet Rec **148:**649–653, 2001

2 Addie DD, Schaap IAT, Nicolson L, Jarret O: Persistance and transmission of natural type I feline coronavirus infection. J General Virol **84:**2735–2744, 2003

3 Battilani M, Coradin T, Scagliarini A, Ciulli S, Ostanello F, Prosperi S, Morganti L: Quasispecies composition and phylogenetic analysis of feline coronaviruses (FCoVs) in naturally infected cats. FEMS Iimmunol Med Microbiol **39:**141–147, 2003

4 Benetka V, Küber-Heiss A, Kolodziejek J, Nowotny N, Hofmann-Parisot M, Möstl K: Prevalence of feline coronavirus type I and II in cats with histopathologically verified feline infectious peritonitis. Vet Microbiol **99:**31–42, 2004

5 Berg AL, Ekman K, Belak S, Berg M: Cellular composition and interferon-g expression of the local inflammatory response in feline infectious peritonitis (FIP). Vet Microbiol **111:**15–23, 2005

6 de Vries AAF, Horzinek MC, Rottier PJM, de Groot RJ: The genome organisation of the Nidovirales: similarities and differences among arteri-, toro- and coronaviruses. Semin Virol **8:**33–48, 1997

7 Fiscus SA, Teramoto YA: Antigenic comparison of feline coronavirus isolates: evidence for markedly different peplomer glicoproteins. J Virol **61:**2607–2613, 1987

8 Foley JE, Poland A, Carlson J, Pedersen NC: Patterns of feline coronavirus infection and fecal shedding from cats in multiple-cat environments. J Am Vet Med Assoc **210:**1307–1312, 1997

9 Freeman AJ, Marinos G, Ffrench RA, Lloyd AR: Immunopathogenesis of hepatitis C virus infection. Immunol Cell Biol **79:**515–36, 2001

10 Gonon V, Duquesne V, Klonjkowski B, Monteil M, Aubert A, Eloit M: Clearance of infection in cats naturally infected with feline coronaviruses is associated with an anti-S glycoprotein antibody response. J Gen Virol **80:**2315–2317, 1999

11 Gunn-Moore DA, Gunn-Moore FJ, Gruffydd TJ, Harbour DA: Detection of FCoV quasispecies using denaturating gradient gel electrophoresis. Vet Microbiol **69:**127–130, 1999

12 Hartmann K: Feline infectious peritonitis. Vet Clin Small Anim **35:**39–79, 2005

13 Herrewegh AAPM, de Groot RJ, Cepica A, Egbering HF, Horzinek MC, Rottier PJ: Detection of feline coronavirus RNA in feces, tissues, and body fluids of naturally infected cats by reverse transcriptase PCR. J Clin Microbiol **33:**684–689, 1995

14 Herrewegh AAPM, Mähler, Hedrich HJ, Haagmans BL, Egberink HF, Horzinek MC, Rottier PJM, de Groot RJ: Persistence and evolution of feline coronavirus in a closed cat-breeding colony. Virology **234:**349–363, 1997

15 Herrewegh AAPM, Smeenk I, Horzinek MC, Rottier PJM, de Groot RJ: Feline coronavirus type II strains 79-1683 and 79-1146 originate from a double recombination between feline coronavirus type I and canine coronavirus. J Virol **72:**4508–4514, 1998

16 Jacobs L, Spaan WJ, Horzineck MC, van der Zeijst BA: Synthesis of subgenomic mRNAs of mouse hepatitis virus is initiated independently: evidence from UV transcription mapping. J Virol **39:**401–406, 1981

17 Jayaram J, Youn S, Collison EW: The virion N protein of infectious bronchitis virus is more phosphorilated than the N protein from infected cell lysates. Virology **339:**127–135, 2005

18 Keck JG, Matsushima GK, Makino S, Fleming JO, Vannier DM, Stohlman SA, Lai MMC: In vivo RNA-RNA recombination of coronavirus in mouse brain. J Virol **62:**1810–1813, 1988

19 Kennedy M, Boedeker N, Gibbs P, Kania S: Deletions in the 7a ORF of feline coronavirus associated with an epidemic of feline infectious peritonitis. Vet Microbiol **81:**227–234, 2001

20 Kim TW, Lee JH, Hung CF, Peng S, Roden R, Wang MC, Viscidi R, Tsai YC, He L, Chen PP, Boyd DAK, Wu TC: Generation and characterisation of DNA vaccines targeting the nucleocapsid protein of severe acute respiratory syndrome coronavirus. J Virol **78:**4638–4645, 2004

21 Kipar A, Bellmann S, Kremendahl J, Köhler K, Reinacher M: Cellular composition, coronavirus expression and production of specific antibodies in lesions in feline infectious peritonitis. Vet immunol immunopathol **65:**243–257, 1998

22 Kipar A, May H, Menger S, Weber M, Leukert W, Reinacher M: Morphologic features and development of granulomatous vasculitis in feline infectious peritonitis. Vet Pathol **42:**321–330, 2005

23 Kiss I, Kecskeméti S, Tanyi J, Klingeborn B, Belak S: Peliminary studies on feline coronavirus distribution in naturally and experimentally infected cats. Res Vet Sci **68:**237–242, 2000

24 Lai MM, Cavanagh D: The molecular biology of coronaviruses. Adv Virus Res **48:**1–100, 1997

25 Motokawa K, Hohdatsu T, Aizawa C, Koyama H, Hashimoto H: Molecular cloning and sequence determination of the peplomer protein gene of feline infectious peritonitis virus type I. Arch Virol **140:**469–480, 1995

26 Motokawa K, Hohdatsu T, Hashimoto H, Koyama H: Comparison of the amino acid sequence and phylogenetic analysis of the peplomer, integral membrane and nucleocapsid proteins of feline, canine and porcine coronaviruses. Microbiol Immunol **40:**425–43, 1996

27 Murphy FA, Gibbs EPJ, Horzinek MC, Studdert MJ: Coronaviridae. *In:* Veterinary Virology, 3rd ed., pp. 495–508. Academic Press, London, England, 1999

28 Pedersen NC, Boyle JF, Floyd K, Fudge A, Barker J: An enteric coronavirus infection of cats and its relationship to feline infectious peritonitis. Am J Vet Res **42:**368–377, 1981

29 Pedersen NC: Virologic and immunologic aspects of feline infectious peritonitis virus infection. Adv Med Biol **218:**529–550, 1987
30 Poland AM, Vennema H, Foey JE, Pedersen NC: Two related strains of feline infectious peritonitis virus isolated from imuncompromised cats infected with a feline enteric coronavirus. J Clin Microbiol **34:**3180–3184, 1996
31 Rosen HR: Hepatitis C pathogenesis: mechanisms of viral clearance and liver injury. Liver Transpl **9:**35–43, 2003
32 Rottier PJM, Nakamura K, Schellen P, Volders H, Haijema BJ: Acquisition of macrophage tropism during the pathogenesis of feline infectious peritonitis is determined by mutations in the feline coronavirus spike protein. J Virol **79:**14122–14130, 2005
33 Stern DF, Sefton BM: Synthesis of coronavirus mRNAs: kinetics of inactivation of infectious bronchitis virus RNA synthesis by UV light. J Virol **42:**755–759, 1982
34 Summers BA, Cummings JF, deLahunta A: Inflammatory diseases of the central nervous system. *In:* Veterinary Pathology, ed. Summers BA, Cummings JF, and deLahunta A, pp. 95–188. Mosby, St. Louis, MO, 1995
35 Surjit M, Kumar R, Mishra RN, Reddy MK, Chow VT, Lal SK: The severe respiratory syndrome coronavirus nucleocapsid protein is phosphorilated and localizes in the cytoplasm by 14-3-3 mediated translocation. J Virol **79:**11476–11486, 2005
36 Vennema H, Poland A, Foley J, Pedersen NC: Feline infectious peritonitis viruses arise by mutation from endemic feline enteric coronaviruses. Virology **243:**150–157, 1998
37 Vennema H: Genetic drift and genetic shift during coronavirus evolution. Vet Microbiol **69:**139–141, 1999
38 Weiss RC, Scott FW: Pathogenesis of feline infectious peritonitis: nature and development of viremia. Am J Vet Res **42:**382–390, 1981

Request reprints from L. Poncelet, Anatomy/Embryology Department, CP 619, Faculty of Medicine, Free University of Brussels, Route de Lennik, 808, B-1070 Bruxelles (Belgium). E-mail: lcponce@ulb.ac.be.